The International Journal Of Engineering And Science (IJES)
|| Volume || 6 || Issue || 2 || Pages || PP 52-61 || 2017 ||
ISSN (e): 2319 – 1813 ISSN (p): 2319 – 1805

The Effect of Arm Stiffness on the Elasto-Kinematic Properties of Single-Axle Suspension by Using the MBS Simulation Model

TOMÁŠ VRÁNA[a], JOSEF BRADÁČ[b], JAN KOVANDA[c], HYNEK PURŠ[d], VOJTĚCH RULC[e]

[a]*Department ofVehicles and Ground Transport, FacultyofEngineering, CULS Prague, Kamýcká 129, 165 21 Praha – Suchdol, Czech Republic*
[b]*Department ofAutomotive Technology, ŠKODA AUTO University, Na Karmeli 1457, 293 60 Mladá Boleslav, Czech Republic*
[c]*University ofWest Bohemia in Pilsen, FacultyofMechanicalEngineering, RTI - RegionalTechnological Institute, Univerzitní 22, 306 14 Plzeň, Czech Republic*
[d]*Advanced Engineering s.r.o., Na Ostrohu16, 160 00 Praha 6, Czech Republic*
[e]*Faculty of Transportation Sciences, Czech Technical University in Prague, Konviktská 20, 110 00 Praha 1, Czech Republic*

----------ABSTRACT----------

The paper is focused on the stiffness analysis of the longitudinal arm of single-axle suspension on elasto-kinematic behaviour of the vehicle axle which is highly important when considering the handling characteristics related tovehicle safety.The elasto-kinematic behaviour of the axle determines the course of the geometrical parameters of wheel suspension, the toe angle and camber as the function of wheel movement during force loading. This paper presents the complex MBS (Multi-Body Simulation)model of the wheel suspension with nonlinear characteristics of rubber-metal bushings. The model also comprises force elements such as springs, shock absorbers, stops and the transverse stabilizer. The model of flexible arm is implemented in the MBS model using the Craig-Bampton method, which represents a flexible body based on the synthesis of its own modal shapes. Subsequently,elasto-kinematic simulations are performed with the help ofthe computational system Hyperwork. The computational part of the paper presents the results of the elasto-kinematic behaviour of wheel axle for the flexible arm with different sheet metal thicknesses (2, 3 and 4 mm) and different materials (steel and aluminium alloy AlSi7Mg). Individual calculation models are compared to each other and also to the model of suspension with therigidarm. Elasto-kinematic analyses are also validated by the measurement inthe testing stage.

Keywords: *wheel axle;flexible arm;nonlinear simulation model;single-axle suspension;wheel geometrical parameters*

Date of Submission: 25 January 2017 Date of Accepted: 20 February 2017

I. INTRODUCTION

Diagrams of geometric parameters such as the vehicle axle toe and camber depending on the vertical motion of the wheel during the impact of external forces define theelasto-kinematic behaviour of the suspension, which has a significant impact not only on the comfort of the vehicle, but also on driving dynamics in the longitudinal, transverse and vertical direction. Thus it directly influences the active and passive vehicle safety and therefore it is necessary to pay attention to it.

But the accurate movement of the wheel is not important only because of driver's direct control. It greatly affects the precision of active assistant systems. From basic systems as ABS or ESP up to systems which will take a place in near future – the systems that will take advantage of intelligent and autonomous cars, which are able to perceive their surroundings. The advanced active systems will be able to adjust suspension's behaviour depending on type or quality of road proactively not only reactively. However without complex knowledge about elasto-kinematic properties of suspension, these systems would be ineffective[1].

Elasto-kinematics is primarily influenced by the deformation characteristics of therubber-metal bushings, but the flexibility of individual supporting elements such as axle arms, subframe, knuckle and bearings also play an important role. Axle suspension is formed by the suspension mechanism with the closed kinematic chain whose number of degrees of freedom *n* can be determined by the equation (1).

$$n = 6 \cdot (u - 1) - 5 \cdot (R + T) - 3 \cdot SP$$

where u is the number of elements of axle suspension mechanism including the frame, R the number of rotational kinematic pairs (KP), T the number of sliding KP and SP the number of spherical kinematic pairs.

For the right functionality of the kinematic mechanism it is necessary to use such a combination of elements, number and type of kinematic pairs, that after the reduction of theoretical parasitic rotations of binary members, n = 1. There are a large number of published kinematic suspension schemes[2,3]. For the analysis and synthesis of such mechanisms in terms of kinematic properties it is possible to use the vector or matrix method [4, 5]. Models with flexible kinematic pairs of basic types of suspension and elasto-kinematic analysis are demonstrated in scientific work [6, 7, 8].

The arm flexibility is solved in scientific work [9]. In the work [10] it was investigated, by the help of elasto-kinematic simulation of MBS model Adams that the knuckle flexibility of wheel suspension causes the difference in the wheel camber of about 40% compared to the rigid model. Parts flexibility has a high impact on results and thus it is not possible to neglect it in some cases. Fig. 1 shows the kinematic scheme of the multilink suspension, where the connection of the longitudinal arm 2 and knuckle 6 can be realized in two different ways. The first possibility is a rotary kinematic pair A2. The second alternative is a fixed connection in points A2h A2d that enforces the defined flexibility of the longitudinal arm 2. The stiffness of the arm in the suspension mechanism causes the preload that influence the rubber-metal bushings and thus it can significantly influence the elasto-kinematic behaviour of the suspension. The aim of this paper is to determine the effect of different stiffness of longitudinal arms on elasto-kinematic characteristics of suspension. Individual variants regarding different arm stiffness are defined in the flexible model by different sheet thicknesses and different type of material. This shows which parameter and how it affects the elasto-kinematic behavior of the suspension during different types of load.The results of the elasto-kinematic behavior of the model with flexible arms are compared with the results of the model containing only rigid arms. The frequent application of this suspension type in the case of sports cars with front-wheel drive, led the authors to analyze its properties and behaviour.

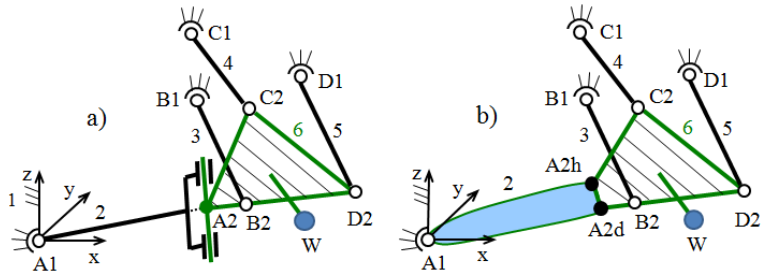

Fig. 1 Kinematical scheme of single-axle suspension, a –rigid longitudinal arm, b- flexible longitudinal arm

II. DEFINITION OF MBS MODEL

MBS model can be defined as an assembly of rigid and/or deformable material bodies which are mutually connected by kinematic coupling allowing their mutual movement (translation, rotation and spherical movement), and it is typically complemented by so-called force elements (springs, shock absorbers, springing wheels stops) . Each element is defined by its mass, inertia and position (kinematic points, center of gravity). The motion equations of rigid elements are built in the HyperWorks system by using analytical methods based on Lagrange equations of mixed type, which can be generally written using the equation (2).

$$\frac{d}{dt}\left(\frac{\partial E}{\partial \dot{s}_j}\right) - \frac{\partial E}{s_j} = Q_j + \sum_{k=1}^{r} \lambda_k \frac{\partial f_k}{\partial s_j} \qquad (2)$$

The usual form (2)of Lagrange equations is also possible to rewrite into the matrix form

$$\frac{d}{dt}\left(\frac{\partial E}{\partial \dot{s}}\right) - \frac{\partial E}{\partial s} = Q + \frac{\partial f^T}{\partial s}\lambda, \qquad (3)$$

where s is the vector of dependent coordinates $s = [s_1, s_2, \dots s_j, \dots s_m]^T$, Q the vector of generalized forces $Q = [Q_1, Q_2, \dots Q_j, \dots Q_m]^T$, f the vector holonomic binding conditions $f = [f_1, f_2, \dots f_k, \dots f_r]^T$ and λ the vector of Lagrange multipliers $\lambda = [\lambda_1, \lambda_2, \dots \lambda_k, \dots \lambda_r]^T$. For the system with n degrees of freedom the rule that the number of dependent coordinates m> n and the number of binding conditions must pay and Lagrange multipliers must be$r = m - n$. The vector of the dependent coordinate s is composed of the position vector of the mass centre of each body of the system $r = [x, y, z]^T$ and the vector whose orientation is determined by the help of Euler angles $\varepsilon = [\Psi, \Phi, \Theta]^T$and thus it is valid that $s = [r, \varepsilon]^T$. The kinetic energy of the whole system $E = E(s, \dot{s}, t)$ is determined as a sum of the kinetic energies of each body established under the König proposition. Furthermore coupling conditions written as the matrix $f = (s, t) = 0$, must be added to Lagrange equations (3) because they are related to the Lagrange multipliers λ. Thanks to the second time derivation of

coupling equation $\ddot{f}(s) = \frac{\partial f}{\partial s}\ddot{s} + \frac{\partial f}{\partial s}\dot{s}$, vector$p_1(s,\dot{s}) = -\frac{\partial}{\partial s^T}\frac{\partial E}{\partial \dot{s}}\dot{s} + \frac{\partial E}{\partial s} + Q$, Jacobi coupling matrix$J = \frac{\partial f^T}{\partial s}$and vector$p_2(s,\dot{s}) = \frac{\partial f}{\partial s}\dot{s}$it is possible to rewrite the equation (3)in the form (4).

$$\begin{bmatrix} H & J \\ J^T & 0 \end{bmatrix} \cdot \begin{bmatrix} \ddot{s} \\ -\lambda \end{bmatrix} = \begin{bmatrix} p_1(s,\dot{s}) \\ p_2(s,\dot{s}) \end{bmatrix} \quad (4)$$

Where His the matrix ofthe weight of the system.

Equation (4) represents the system of differential-algebraic equations that is difficult to solve analytically. In the multi-body mathematical environment HyperWorks, the Lagrange equations are solved on the basis of numerical analysis using the DSTIFF integrator which is based on the DASPK method.

III. ELASTO-KINEMATIC MODEL OFSINGLE-AXLE SUSPENSION

The Multi-body model of multi-arm suspension of the vehicle in two basic versions was created in the MotionViewmoduleinthe HyperWorks simulation environment. The elasto-kinematic model of suspension (Fig. 2 left) was firstly formed according to a simpler kinematic diagram (Fig. 1 a).

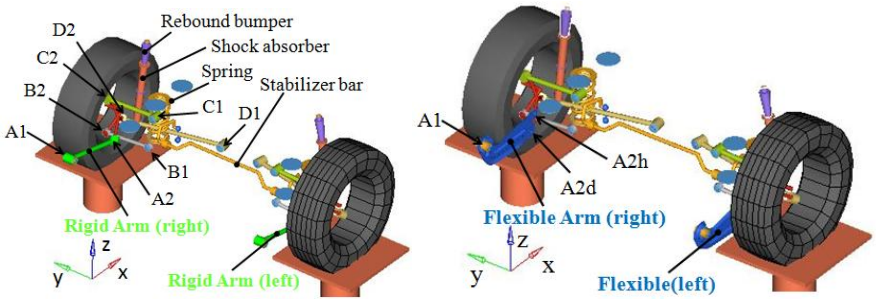

Fig. 2 Elasto-kinematic model of multi-arm suspension with flexible bushings and rigid longitudinal arms (left - green), model with flexible bushings and arms (right - blue)

This model consists of absolutely rigid bodies, which are interconnected by flexible kinematic pairs representing rubber-metal bushings. The geometric position of kinematic pairs of the suspension mechanism in the global coordinate system (GCS) is shown in Table 1.

Tab. 1 Position of kinematic pairs in the absolute coordinate system

Coordinate in GCS	Point of suspension kinematic pair							
	A1	A2	B1	B2	C1	C2	D1	D2
x [mm]	2,098	2,402	2,480	2,502	2,534	2,534	2,805	2,790
y [mm]	-603/603	-595/595	-395/395	-678/678	-380/380	-685/685	-105/105	-685/685
z [mm]	36	-33	-21	-40	143	130	-10	-45

The longitudinal arms (Fig. 2 left - green), but also other arms and axle parts, such as e.g. knuckle or subframe are rigid. The elastic behavior of the rubber-metal bushing of the axle is generally described by six non-linear deformation characteristics. It is the radial deformation characteristic Dx = f (Fx),Dz = f (Fz), axial characteristic Dy = f (Fy), moment characteristics,cardanicφz = f (Mz),φx = f (Mx) and torsion φy = f (My). These characteristics were required during the assemblyof the model of axles for each suspension bushing and were subsequently experimentally measured. The characteristics were measured according to the loading modes defined in Fig. 3.

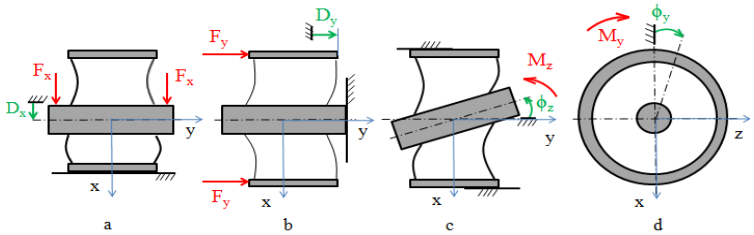

Fig. 3 Loading modes for measuring deformation characteristics of flexible suspension bushing (a - radial deformation characteristics, b - axial deformation characteristics, c - cardanic deformation characteristics, d - torsion deformation characteristic)

As an example of the measured deformation characteristics, the torsion φy = f (My) and radial Dx = f (Fx) deformation characteristic of the bushing in the kinematic point A1 is introduced in Fig.4.

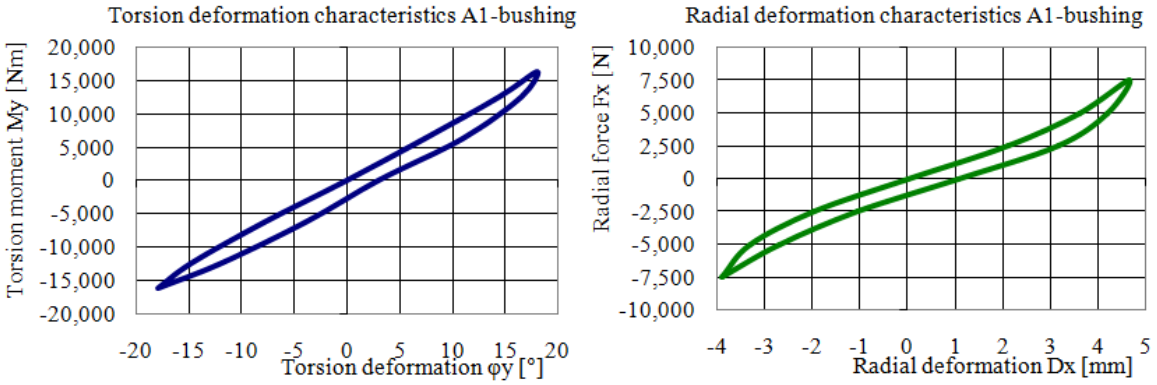

Fig.4 Deformation characteristics A1-rubber-metal bushing, torsion(blue), radial in x axis (green)

The creation and optimization of the model of suspension with rigid body and kinematic pairs was followed by the extension of the model of flexible arms (Fig. 2 right - blue). Moreover, the type of kinematic couplings between the flexiblearmand knuckle had to be modified from the roller type to the fixed type that guarantees optimal kinematic performance of the suspension mechanism. Other input data of the model, as the position of kinematic pairs, body weight andelasto-kinematic characteristics of bushings, remained consistent with the first variant.

3.1 Computational model of suspension flexible arm

In order to analyze the effect ofelasto-kinematics properties,the suspension flexible longitudinal arms were created in different sheet metal thicknesses 2; 3 and 4 mm and in two material variants - steel and aluminium alloy AlSi7Mg.The mechanical properties of both materials are shown in Table2. The model of arm made of steel with the thickness of 3 mm is regarded as basic, and its simulation results were verified experimentally.

Tab.2 Mechanical properties of the arm material[11]

Material	Density ρ [kg/m^3]	Poisson μ [-]	Modulus of elasticityE [MPa]
Steel	7,860	0.3	$2.1 \cdot 10^5$
AlSi7Mg	2,700	0.33	$0.74 \cdot 10^5$

To create the arm model and implement it into the MBS model of axles,it is necessary to develop the corresponding CAD data in the surface model form. The MKP Pre-processor system Hypermesh of the HyperWorks system was used in this case. In this calculation module the weight and static bending stiffness of the individual variants of arms was also calculated. On the surface geometric model, the classical FEM combined network of triangular and quadrilateral elements PSHELL type of 10 mm was developed (Fig. 5).

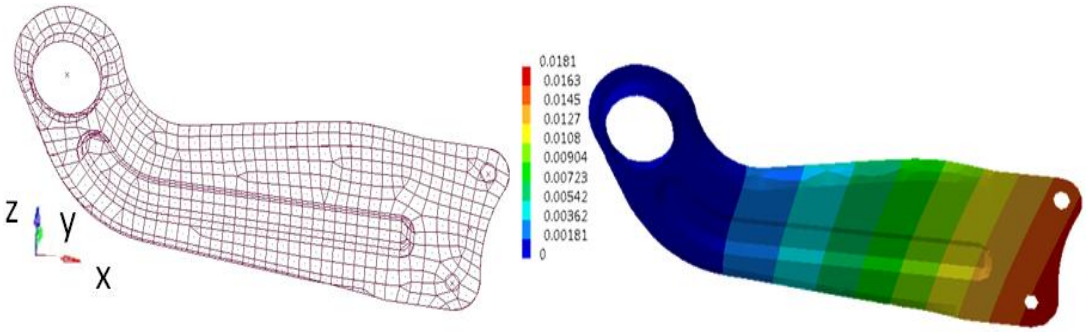

Fig.5 MKP mesh of the arm computational model(left) and deformation[mm] during loading with the unit force [N] (right)

The material thickness and the material type according to different options were assigned to all the elements. The model was subsequently supplemented by the boundary conditions (placement) and loaded by the unit loading force in Y-axis direction. The calculated static stiffness and weight is listed in Table 3.

Tab.3 Computed weight and static stiffness of longitudinal arm

Material	Steel			AlSi7Mg		
Plate thickness [mm]	2	3	4	2	3	4
Weight [kg]	0.89	1.55	2.21	0.30	0.53	0.76
Static stiffness [N/mm]	10.1	30.9	60.1	3.6	11.0	21.5

Repeated calculation of the arm stiffness forthe FEM net with smaller elements of 5 mm showed the same results as the original network with 10 mm. It is evident that the selected network is optimal for calculation in terms of precision of results and computational time productivity. The flexible model ofthe longitudinal arm was created for theelasto-kinematic calculations by the synthesis of modal shapes using the Craig-Bampton method. The real body in its finite representation (FEM model) is discretized using a finite number of degrees of freedom. The modal reduction using Craig-Bampton approximates linear displacements of the nodes uby the linear combination of modal shapes (self-vectors) κ_i, that describe the dynamic behaviour of the body and the modal coordinate q_i according the equation (5), where l denotes the number of modal shapes.

$$u = \sum_{i=1}^{l} \kappa_i \cdot q_i(t) \qquad (5)$$

Equation (5) can be rewritten in thematrix form (6).

$$u = K \cdot q(t). \qquad (6)$$

A full approximation of the real deformation of the body can be theoretically achievedby the infinite number of modal shapes of the body, but sufficiently accurate compensation can be relatively achieved at a low number of shapes. This means that the modally elastic body is computationally more efficient compared to the conventional FEM model used in common practice for the stress-strain analysis. The definition of the small linear deflection of the modally flexible body extends to its local coordinate system (LCS), which together with the body mechanism of coupled bodies in MBS model, performs complex movements with respect to GCS. According to Fig. 6 it is possible to use the transformation matrix T_{0b} to determine the position vector of the flexible body r_{fl} (7) which is completed by the vector of modal shapes u in comparison with the classical position vector r for the rigid body. These position vectors are possible inputs into the vector s when completing the Lagrange equations (3).

$$r_{fl} = r_{Ob} + T_{0b} \cdot (r_T + u) \qquad (7)$$

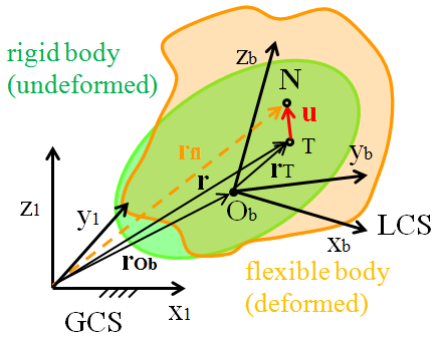

Fig.6 Description of flexible body in GCS

Tab. 4 First six natural-frequencies of longitudinal arm, different material and plate thickness

Material	Plate thickness [mm]	Natural frequency [Hz]					
		1	2	3	4	5	6
Steel	2	129.9	244.9	419.7	479.9	714.9	805.5
	3	200.1	302.0	576.1	657.2	973.5	1,096.3
	4	261.73	343.6	698.7	799.8	1,189.9	1,344.0
AlSi7Mg	2	131.1	248.8	425.8	486.8	727.3	743.9
	3	201.5	306.5	584.4	665.4	989.4	1,112.0
	4	263.8	348.3	708.5	808.6	1,209.0	1,362.2

The required number of modal shapes needed to describe the deformation behaviour of the elastic body is determined by the modal analysis. The calculated values of natural-frequencies of the longitudinal arm of different variants using the HyperWorks software are shown in Table 4. The first three modal shapes for the arm made of steel with the plate thickness of 5 mm are shown in Fig. 7.

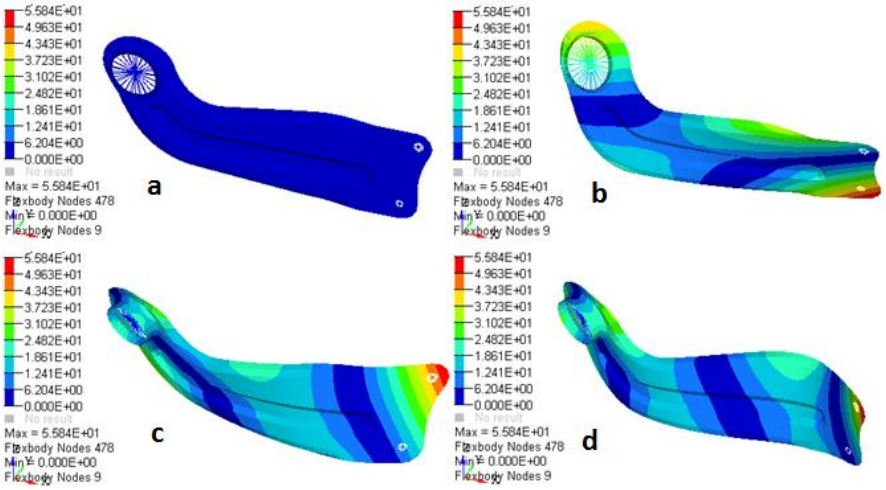

Fig. 7 The first three modal shapes of the longitudinal arm of suspension - variant steel, thickness 5 mm, a - non-deformed state ; b - the first modal shape (torsion around the longitudinal axis of the arm); c - the second modal form (bending); d - the third modal shape (bending), color scale indicates the deformation field [mm]

Because the ratio of the modulus of elasticity E and the density ρ for steel and aluminiumalloy AlSi7Mg is nearly the same, the behavior of longitudinal arms under the dynamic loading will be very similar. Calculated values of natural-frequencies of longitudinal arms for both materials confirm this statement. However the behavior of these materials at quasi-static loading in which the modulus of elasticity E is decisive factor can be different and may influence the elasto-kinematic characteristics of the suspension.

3.2Implementation of flexible armin MBS model of suspension

The created modal flexible models of longitudinal arms were connected with the surrounding parts of the MBS model, using the so-called RBE2 Spiders. This entity generates the interface-coupling between the independent node (kinematic point) of the MBS model and dependent nodes of the flexible model. On the model of flexible arm there are three RBE2 Spiders (Fig. 8). First RBE2-1 (node number 926) connects the kinematic point A1 with 44 nodes on the inner surface of the arm. The second RBE2-2 (node 927) and the third RBE2-3 (node 928) connects the A2h and A2d points with five and four nodes on the perimeter of holes (longitudinal arm-knuckle).

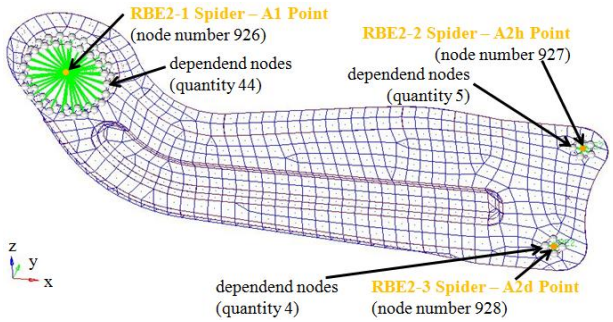

Fig.8 RBE2 Spiderscreatedon the model of longitudinal arm (left side)

3.3Definition of loading modes

Three loading modes of the wheel suspension with different variants of the longitudinal arms were defined in the MBS model. There were used loading modes in the MotionView module for kinematic and elasto-kinematic calculations which were predefined in the HyperWorks software.The intended load is implemented into the system of suspension with the defined movement of wheels support. In the first mode it simulates the vertical movement of the support wheels motion from the lower to the upper stopcaused by vertical respectively radial force FV. The wheel travel was set in the interval$W_Z = \langle -105; 105 \rangle$ mm. The other two modes transferthe forces in lateral and longitudinal directions, which help to analyze the elasto-kinematic behavior of the suspension when cornering and braking. For the lateral force it was chosen the interval $FL = \langle -10{,}000; 10{,}000 \rangle$N and for the longitudinal braking force the interval $FB = \langle 0; 10{,}000 \rangle$N. Simulations were calculated in the time period 0 s to 80 s using the step of 0.05 s.The time dependence of the vertical force FV, the longitudinal braking force FB and lateral force FL are shown in Fig. 9. In the time interval from 0 s to

20.4 s the wheel is affected only by the vertical force FV. The wheels of suspension move first in parallel compression and then in standard compression, in which is reflected the effect of the stabilizer causing higher difference in vertical forces on both wheels. Another loading mode is in the interval from 20.4 s to 40 s when the wheel is affected only by lateral force FL in sinusoidal wave. Finally, from 60 s to 70 s the longitudinal braking force FB affects the wheels. The effect of FL force in the defined interval causes dependent changes in the FV and FB force. The same is valid for the longitudinal braking force FB.

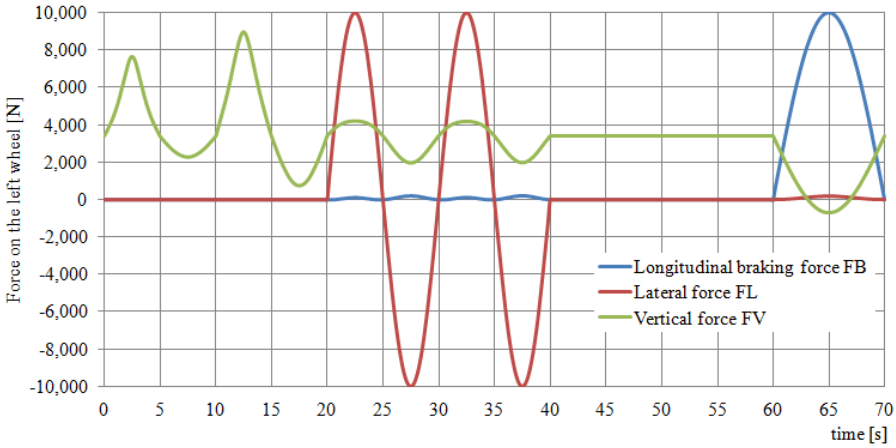

Fig. 9 Time dependence of vertical force FV, longitudinal braking force FB and lateral forces FL on the left wheel during the elasto-kinematic simulation

IV. VALIDATION OFMBS MODEL ON THE BASIS OF EXPERIMENTAL MEASUREMENT

The results of the simulations carried out in the MBS computational model of the axle suspension were validated by experimental measurements. To measure the behaviour of the geometric parameters (toe, camber) of the axle suspension depending on the wheel travel a measurement of the axle geometry on the testing device Beissbarth VAG 1995 + VAS5080 type was used (Fig. 10). On the outer profile of the wheel rim, the measuring heads set in the horizontal position were fixed using the three-point bracket. Each head contains two CCD cameras that use infrared beams projected on the wheel and measure the geometric parameters of the suspension. CCD cameras with transceiver function also provide communication between the heads of each individual wheel. Measuring in the horizontal and vertical plane provides one measurement system that allows compensation of the shimmy. Before the measurement, the whole measuring system was calibrated. The measured data are sent to the computer controlled measuring station. Measured vehicle was loaded and unloadedin intervals of movement of the rear wheels $W_Z = \langle -100; 100 \rangle$with the step of 10 mm. At each position the toe angle $\delta = f(W_Z)$ and the camber $\gamma = (W_{Z)}$ were monitored. Each wheel was placed on the sliding pad which allows, due to the variable load during the vertical motion of the wheel, also side movement. This increases the accuracy of measuring the values. The variant of axle suspension with the longitudinal arm made of steel with the thickness 3 mm was experimentally measured.

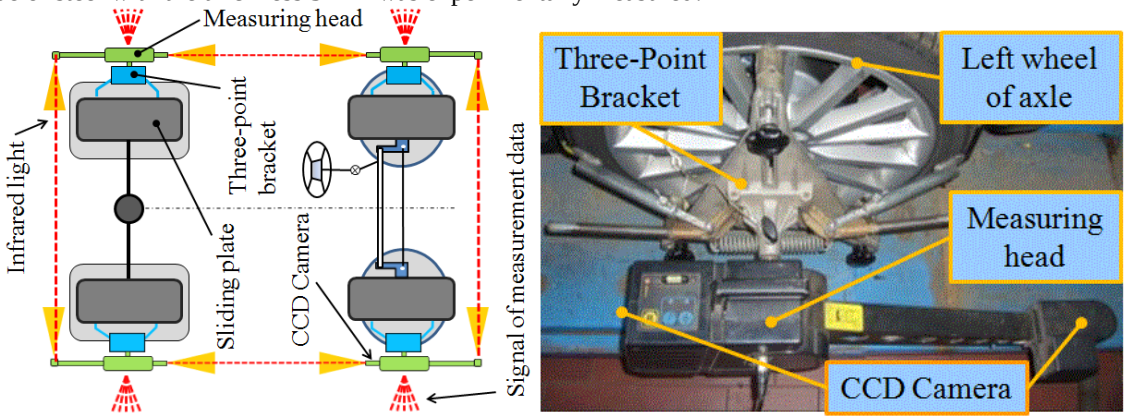

Fig.10 Schematic view of measurement of suspension geometry on testing machineBeißbarth VAG 1995 + VAS5080 (left), measuring head on the left wheelduring experiment (right)

V. RESULTS OF SIMULATION CALCULATIONS

5.1 Effect of flexible armon elasto-kinematicsby wheel travel

The basic view of the elasto-kinematic characteristics of the suspension is given by the wheel toe and camber values depending on the movement of the wheels W_z in the vertical z-axis direction (Fig. 11).

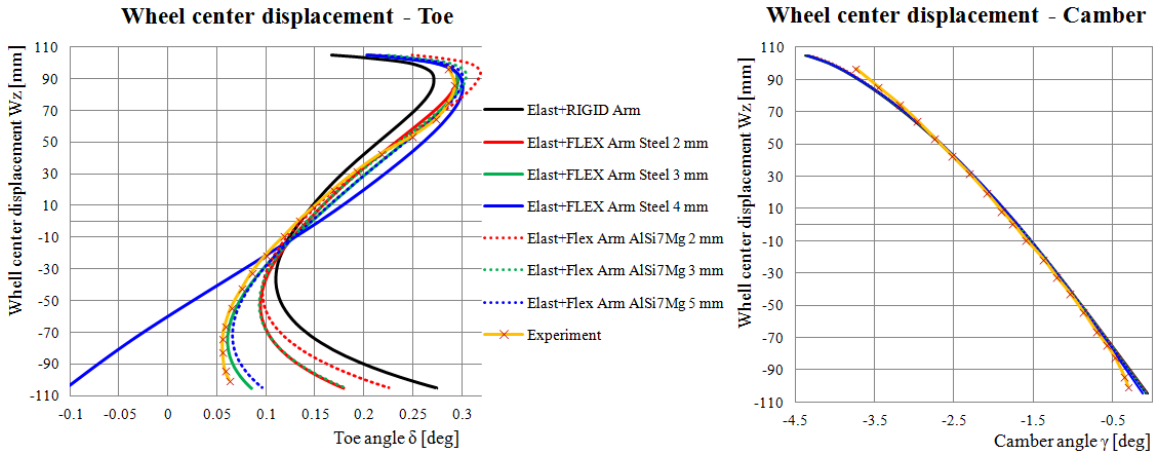

Fig. 11 Wheel toe angle [deg] and camber [deg] vs.wheel-centre movement [mm] in z-direction

These dependences show that both kinematic diagrams of the suspension (Fig. 1) at the different bending stiffness of the longitudinal arm strongly affect only the wheel toe. The behavior of the wheel camber is consistent for both options. Curves of toe angle δ have the shape of an inverted S. For $W_Z = 0 - 90$ mmthe dependence is approximately linear which is very advantageous in terms of handling when driving in the curve. The experimentally measured toe and camber behavior correspond to simulation very well, the difference arises only in areas of the upper and lower stop, the position of the wheel$W_Z = -90$, respectively 90 mm. The calculated values of the wheel toe $\delta = f(W_Z)$are for all generated models of suspension summarized in Table5.The elasto-kinematic model with the rigid arm (Fig. 1a) shows significantly different toe values against the model with the flexible arm (Fig. 1b) made of steel with the thickness of 3 mm, especially for higher negative valuesofW_Z.For$W_Z = -88.65$ mm the difference is in the toe for both models 84.6 %. For $W_Z = -77.88$ mm is then 68.9 %. For the upper area of the wheel position$W_Z = 77.88$ respectively 88.65 mm the difference is considerably lower, concretely 9.25 % and 8.1 %. The difference in the toe is negligible e.g. for $W_Z = -88.65$ mm where it is 7.5%. Conversely, the biggest difference is found in the lower stop and thus 37.3 %. It is evident that for the precise determination of the toe it is necessary to use the MBS model of the suspension with a flexible longitudinal arm. On the other hand, in case of the wheel camber it is important only in calculations of the lower stop; otherwise the computationally simpler MBS model with rigid arm can be used.

Tab. 5 Computed values of wheel toe in defined wheels positions

Wheel centre displacement in W_Z [mm]	Toe angle [deg]				
	-88.65	-71.88	0	71.88	88.65
ELAST+RIGID arm	0.130	0.103	0.142	0.276	0.295
ELAST+FLEX steel 2 mm	0.196	0.146	0.135	0.255	0.272
ELAST+FLEX steel 3 mm	0.065	0.061	0.146	0.281	0.296
ELAST+FLEX steel 4 mm	-0.069	-0.031	0.154	0.293	0.300
ELAST+FLEX AlSi7Mg 2 mm	0.159	0.118	0.136	0.287	0.316
ELAST+FLEX AlSi7Mg 3 mm	0.132	0.104	0.142	0.281	0.304
ELAST+FLEX AlSi7Mg4 mm	0.073	0.066	0.146	0.284	0.301

The arm made of steel with the thickness of 2 mm has nearly the same behavior as the arm made of AlSi7Mg with the wall thickness of 3 mm. The advantage is that the arm of aluminium alloy offers weight saving - 0.72 kg per vehicle. The arm made of steel with the thickness of 4 mm shows different toe values in comparison with other variants. During $W_Z < 61.13$ mm causes unwanted toe-out.The presented weight savings when using longitudinal arms of AlSi7Mg will be in case of real design lower due to the lower energy absorption of this material during crash which must be taken into account. To achieve the same behavior of AlSi7Mg arms as steel arms, the lower modulus of elasticity has to be compensated by increasing the wall thickness.

5.2 Effect of flexible armon elasto-kinematics by loading

The influence of individual variations of longitudinal arms on elasto-kinematic suspension characteristics during lateral and longitudinal braking force is shown in Fig. 12 and Fig. 13. These are dependences of δ = f(FL, FR), and γ = f(FL, FR). Between the two basic models (rigid arm vs. flexible arm - steel with the thickness of 3 mm) there are for FL = 9,000 N the difference in the toe angle 3.1% and 1.5% in camber. The toe angle increases linearly during the action of side forces, which results in the stable behavior of the vehicle when cornering. For FL > 0 the toe angle is mostly changed in the case of AlSi7Mg arm with the thickness of 2 mm, and for δ = 0.135 deg to 0.961 deg. For FL < 0 deg it is then from 0.135 to - 0.502 deg. The smallest change in toe causes the steel arm with the thickness of 5 mm.

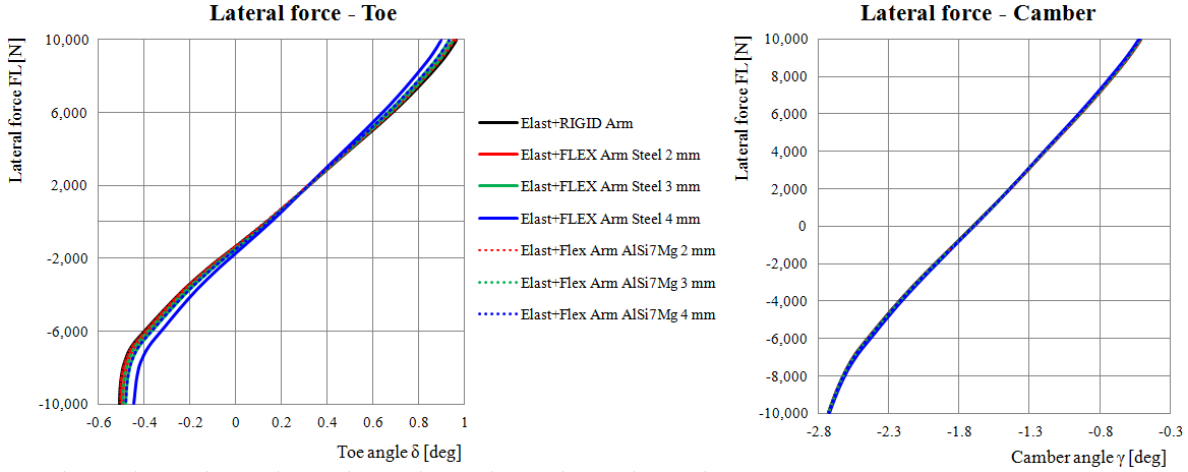

Fig. 12 The change of toe angle δ and camber γ during action oflateral force FL

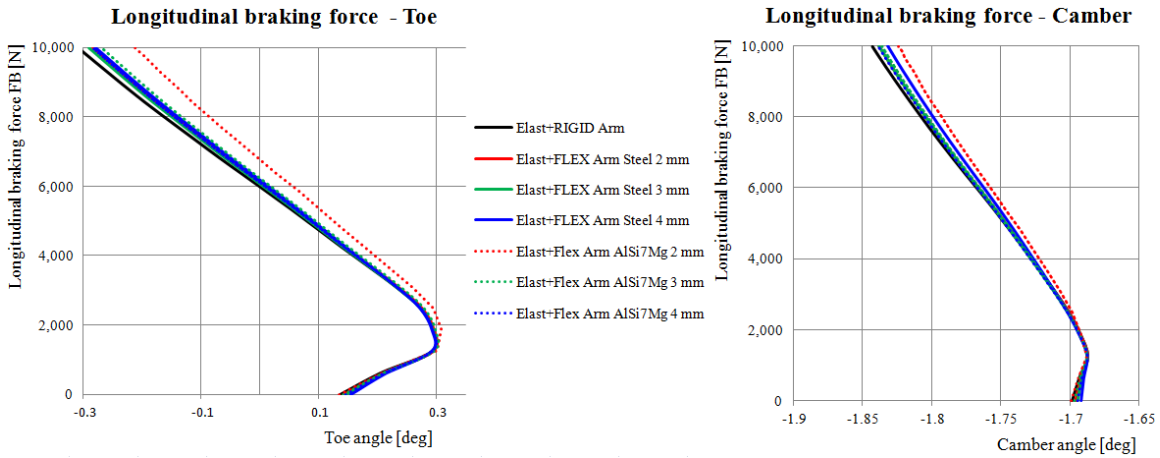

Fig. 13 The change of toe angle δ and camber γ during action of braking force FB

The effect of the stiffness of the longitudinal arm on the geometrical position of the wheel under the action of the longitudinal braking force is shown in Fig. 13. The wheel toe increases with the longitudinal force FB, e.g. for steel arm with the thickness of 3 mm up to δ = 0.295 deg for FB = 1,226 N. Furthermore, by increasingload it decreases and changes in toe-out (FB = 5,877 N). The smallest absolute decline of the wheel toe was calculated for the variant with the flexible arm AlSi7Mg and the thickness of 2 mm, while the biggest decrease was calculated for the rigid arm and thus 0.439deg.

Similarly, it is possible to describe the change in the wheel camber that with increasing the braking force, increases up to the limit FB = 1,253 N and further drops. For the whole loading interval, the camber angle varies from -1.69 to -1.84 deg. Furthermore, it appears that for FB = 9,000 N the toe angle is for the model with rigid arm by 7.6 % lower compared to the flexible arm (steel, 3 mm). The camber angle is lower of about 0.5%.

VI. CONCLUSION

The paper is devoted to the impact of longitudinal arm stiffness of single-axle suspension on elasto-kinematic properties of the vehicle axle, which is important for an accurate analysis that has great influence on right performance of active assistant systems. For this purpose the computational model was created in the HyperWorkssoftware for several variants of the longitudinal arm stiffness. The created computational model includes all the basic force elements, such as springs, shock absorbers, stops, stabilizer, and also the deformation characteristics of rubber-metal bushings which were measured on the experimental station. This enables a correct setting and validation of the computational model. Computational models of individual variants of flexible arm were created by the synthesis of modal shapes using the Craig-Bampton method and then implemented in the MBS modem. The main output of simulations is the development of the toe and camber angle according to the vertical movement of the wheel centre and force loading in the lateral and longitudinal direction. The elasto-kinematic model with the rigid longitudinal arms showed significantly different values of the toe angle against the model with flexible arms, especially in the area of negative wheel travel. The results also show that for the precise determination of the toe it is important to use the MBS model of axle suspension with the flexible longitudinal arm. Conversely, in case of the wheel camber it is important only in case of calculations of the lower stop. In other cases it is possible to recommend computationally simpler MBS model with the rigid arm. Simulations also show that the self-stiffness of the arm highly influences the behavior of the wheel toewhich was also confirmed by repeated calculations of individual variants. Less influence can be seen in the light of the toe angle and camber under the effect of the longitudinal braking force.

REFERENCES

[1] Kanarachos S, Kanarachos A. Intelligent road adaptive suspension system design using an experts' based hybrid genetic algorithm. Expert Systems with Applications. 2015; 42(21): 8232-42.
[2] Apetaur M, Stejskal V. Motor Vehicles VI - Suspension theory. 1st ed. Prague: CTU; 1983.
[3] Schramm D, Hiller M, Bardini R. Modellbildung und Simulation der Dynamik von Kraftfahrzeugen, Duisburg: Springer-Verlag Berlin Heidelberg; 2010.
[4] Brát V. Matrix methods in analysis and synthesis of shape mechanical systems, Prague: Academia; 1981.
[5] Simionescu PA, Beale D. Synthesis and analysis of the five-arm rear suspension system used in automobiles: Mechanismand Machine Theory. 2002 Sept; 37(9): 815-832.
[6] Hiller M, Woernle C.Elastokinematical analysis of a five-point wheel suspension:SIA-JournalofIngénieurs de l´automobileJg.1985; 77-80
[7] Knapczyk J, Dzierzek S. Displacement and force analysis of five-rod suspension with flexible joints: Trans. ASME, Journal of Mechanical Design.1995 Dec; 117:532-538
[8] Kang JS.Elastokinematic analysis and optimization of suspension compliance characteristics: SAE International - technical paper 970104.1997 Jan.
[9] Knapczyk J, Maniowski M. Stiffness synthesis of a five-rod suspension for given load-displacement characteristics: Proceedings of the Institution of Mechanical Engineers. 2006 Jul; 220: 879-889.
[10] Heissing B, Ersoy M. Fahrwerkhandbuch, Wiesbaden:Vieweg +Teubner Verlag, 2008.
[11] Michalec J. Flexibility and strength I. Prague: CTU; 1995.